J. For. Res. (2022) 33:1925–1937
https://doi.org/10.1007/s11676-022-01456-7

ORIGINAL PAPER

Overexpression of the *PdpapERF109* gene enhances resistance of *Populus davidiana* × *P. alba* var. *pyramidalis* to *Fusarium oxysporum* infection

Jian Diao[1] · Mingrui Li[1] · Ping Zhang[1] · Cheng Zong[2] · Wei Ma[3] · Ling Ma[1]

Received: 20 April 2021 / Accepted: 15 December 2021 / Published online: 10 April 2022

Abstract The key transcription factor gene *PdPapERF109* was cloned from *Populus davidiana* × *P. alba* var. *pyramidalis* (Pdpap), and after overexpression of *PdPapERF109* in transformants, the gene functions in the resistance response to *Fusarium oxysporum* infection. Compared with the wild Pdpap, after inoculation with *F. oxysporum*, the physiological and biochemical characteristics, including relative fresh weight, peroxidase activity, and the percentage of electrolyte leakage showed that, after overexpression of the *PdPapERF109* gene, the transformants grew well and displayed significant resistance to *F. oxysporum* infection. By comparing the reactive oxygen species scavenging capacity of Pdpap plants after pathogen infection, the *PdPapERF109*-overexpressing plants had significantly better reactive oxygen species scavenging ability than the wild plants. Comprehensive analysis of plant morphology and various physiological and biochemical parameters showed that the overexpression of the *PdpapERF109* gene significantly improved the resistance of Pdpap plants to *F. oxysporum* root rot. Therefore, increasing the expression of the homologous *ERF109* gene can be an effective strategy to increase disease resistance in hybrid poplars.

Keywords ERF · *Fusarium oxysporum* tolerance · Gene over-expression · Genetic transformation · Transcription factor

Introduction

Populus is a genus widely distributed around the world, and many species are highly adaptable to various environmental conditions. As a model species for woody plant research (Ning et al. 2018), *Populus* has the advantage of having a smaller genome (480 Mb) (Cossu et al. 2012), and that efficient genetic transformation systems are available for different species (Maheshwari and Kovalchuk 2016). A reason why *Populus davidiana* × *P. alba* var. *pyramidalis* Louche

Corresponding editor: Tao Xu.

Jian Diao and Mingrui Li have contributed equally to this work.

Project funding: The work was supported by the Central University Basic Research Business Expenses Special Fund Project [grant number: 2572018AA37] and the Fundamental Research Funds for the Central Universities [2572019CP01].

The online version is available at http://www.springerlink.com.

Wei Ma and Cheng Zong are co-corresponding authors.

Supplementary Information The online version contains supplementary material available at https://doi.org/10.1007/s11676-022-01456-7.

✉ Cheng Zong
moredonkey@163.com

✉ Wei Ma
mawei@hljucm.net

✉ Ling Ma
maling63@163.com

[1] College of Forestry, Northeast Forestry University, Harbin, People's Republic of China

[2] College of Wildlife and Protected Area, Northeast Forestry University, Harbin, People's Republic of China

[3] College of Medicine, Heilongjiang University of Chinese Medicine, Harbin, People's Republic of China

(PdPap) is suitable as an urban species is that it has a male vegetative breeding system (Yao et al. 2018). After blooming in spring, no catkins are formed so it can be used as a choice of urban tree species in north China (Yao et al. 2018). Studies have confirmed that the hybrid tolerates low temperatures and drought (Qin et al. 2005; Zhao et al. 2015). However, due to deteriorating environmental conditions in recent years, the hybrid is facing increasingly challenges to growth and development from pathogenic microorganisms (Yu et al. 2019), temperature extremes (Zhao et al. 2015), moisture extremes or deficits (Qu et al. 2014) and ion concentrations (Lu et al. 2004; Chen et al. 2020) that can result in different degrees of damage. Among the many hazards, root rot is one of the most serious and devastating diseases and has attracted widespread attention (Moncrief 2010). Once the disease breaks out, it will cause large-scale root rot and death (Ikeda et al. 2005). Xie et al (1993) was the first to report on the damage status, symptom characteristics, and infection pathways of *Fusarium oxysporum* in *Populus*×*euamerica* (Dode) Guinier that occurred in the Dongting Lake area. Reports note that *F. oxysporum* has been used for the infection of *Populus trichocarpa* (Zadworna et al. 2014) and Pdpap (Guo et al. 2020).

Fusarium oxysporum is one of the main pathogenic species of the *Fusarium* genus, and infects many types of plants, eventually causing root rot and plant wilt (Puhalla 2011). In addition to being parasitic on the host plant, *F. oxysporum* also survives in soil and in the air, and after 10 years of survival, it may still be strongly pathogenic (Wu et al. 2009). The first physical barrier to be breached by *F. oxysporum* in plant infection is the plant cell wall (Huang 2001). The degradation of the cell wall is achieved by secreting cellulase, pectinase, and β-glucosidase enzymes (Li and Zhang 2010). The pectin produced after degradation of the cell wall blocks the ducts of the host plant (Florendo et al. 2003), which hinders the absorption of water and eventually causes the plant to wilt and die (Miedes et al. 2013). *Fusarium* acid (5-butyl-2-picolinic acid) secreted by *Fusarium* enhances the permeability of the root cell membranes causing serious damage (Wang and Ng 1999). In addition, the acid will also reduce the active oxygen content in mitochondria, ultimately hindering the water absorbing function of plant roots and inhibiting plant growth (Lu et al. 2004). In addition, the presence of pedigree-specific regions makes the *F. oxysporum* genome highly susceptible to horizontal transfer (Bootsma et al. 2000), resulting in the formation of novel specialized types and physiological races of the pathogen (Köppl and Carr 2003), giving *F. oxysporum* a wide host range and extremely strong pathogenicity (Ma et al. 2013).

Transcription factors are closely related to the plant stress response (Sakuma et al. 2002). The process by which transcription factors enhance the ability of plants to resist stress is mainly a result of the increased expression of transcription factor genes in response to stress (Ali et al. 2013), and this can then further regulate the expression of downstream functional genes (Stein et al. 2001; Hou et al. 2009). Zeng and Mu (2016) have shown that transcription factors play a vital role in plant stress resistance, and the expression of this stress resistance function is usually coordinated under the common regulation of many transcription factors (Sun et al. 2009). In addition, the adaptation of plants to adverse environmental conditions can be achieved by generating secondary metabolites (Stangarlin et al. 2011). When their growth status is disturbed, secondary metabolites will increase the tolerance of plants to stress (Makkar et al. 2007). Studies have shown that different types of transcription factors can jointly participate in the regulation of plant secondary metabolite biosynthesis through synergistic effects (Wasternack and Strnad 2019), which then respond to an adverse environment.

The largest transcription factor family is the APETALA2/ethylene-responsive factor (AP2/ERF) (Xue and Loveridge 2010), which effectively responds to biotic or abiotic stresses during the process of adaptation, thereby mobilizing various resistance response genes (Zorrilla et al. 2014). Ethylene response factors (ERFs) are a family of transcription factors unique to plants (Qiu et al. 2012), and named because *ERF* genes can respond to ethylene stress to a certain extent (Mizoi et al. 2012). Different types of ERF transcription factors have different gene expression regulation. For example, ERF transcription factors can simultaneously activate or inhibit expression of genes related to disease control (Fujimoto et al. 2000). In addition, since there is no GCC-box element in the promoter of genes involved in the regulation of maturation and senescence (Jin et al. 2010), ERF transcription factors work together with other types of cis-acting elements (Takagi et al. 2020). Based on the results of published research, there are several ways in which ERF transcription factors function in the process of stress resistance: (1) through direct regulation of PR gene expression; (2) via indirect regulation of key gene expression in hormone synthesis pathways (Mader and Cameron 2006); and, (3) in combination with the promoters of key genes to regulate gene expression and the expression of secondary metabolites (Kagaya et al. 1999). The ERF transcription factor family plays a powerful role in many diverse life activities, including positive responses to biotic/abiotic stresses, growth, and metabolite regulation (Mizoi et al. 2012). ERF member genes respond to stresses, including pathogenic microorganism infection (Shi et al. 2015), temperature extremes (Dossa et al. 2016), ion concentrations, and mechanical damage (Licausi et al. 2013). At the same time, the ERF family, as an important regulatory center of the responses to various types of stress, can comprehensively integrate hormone signals such as jasmonic acid and ethylene (Müller and Bosch 2015). In addition, the heterologous expression of the ERF

family member genes can produce different degrees of resistance to various stresses through the activation of resistance pathways (Yi et al. 2004).

Based on the results of previous research on transcriptome data (Diao et al. 2021), the transcription level of Pdpap infected with *F. oxysporum* is well understood. The transcriptome data was screened with the standard of $\log_2$ (Fold Change) > 4 and *P* adj < 0.05. Based on this, genes were obtained in Pdpap, whose transcription levels continued to increase after infection (Supplementary Table S1). Among these genes, there are three typical transcription factors (ERF109, ERF6, MYB41). Among them, *ERF109* is basically at the highest level and therefore an in-depth analysis was carried out on *ERF109*.

The 809 bp cDNA of the *PdPapERF109* gene was isolated from Pdpap. The recombinant vector pBI121-*PdPapERF109* for the over-expression of *PdPapERF109* was constructed under the control of the CaMV 35S promoter, and it was successfully transformed into Pdpap. In addition, evidence based on the analysis of molecular, morphological, and physiological data showed that the *PdPapERF109*-overexpressing transformants have enhanced resistance to *F. oxysporum* CFCC86068. The objectives of this study were to determine the function of the *PdPapERF109* gene in resistance to *F. oxysporum* infection using physiological and biochemical methods to provide a contribution to improving plant disease resistance in hybrid poplars.

Materials and methods

Materials

Wild Pdpap seedlings were cultured on 0.5×MS (Murashige and Skoog) medium supplemented with 0.01 mg/mL 1-naphthaleneacetic acid (NAA). For stable gene transformation, leaves from 1-month-old plants were transferred to differentiation medium that contained 0.5 mg/mL 6-benzylaminopurine (6-BA), 0.1 mg/mL NAA, and 0.02 mg/mL thidiazuron (TDZ). The tissue cultures were grown in a tissue culture room (Zhang et al. 2009). The seedlings obtained by redifferentiation are transferred to 0.5×MS medium. In order to simulate growth under natural conditions, the seedlings were transplanted to artificial soil and cultivated in an controlled environment at 22 ± 2 °C with a light intensity of 400 lx/m^2/s, a photoperiod of 16 h light and 8 h dark, and a relative humidity of 65–75% (Lu et al. 2011).

The strain of *F. oxysporum* CFCC86068 was obtained from the China Forestry Culture Collection Center. The pre-activated *F. oxysporum* was transferred to PDA medium and cultured in dark for 7 days. A 9 mm-diameter borer was used to punch holes at the edge of the hyphae and transferred to a new PDA medium. After culturing at 28 °C for 14 days, spores were washed five times with sterile water, filtered through eight layers of gauze and collected into a 50 mL centrifuge tube. Spore density was calculated using a hemocytometer and stored at room temperature for later use.

RNA extraction and cDNA transformation

Total RNA was extracted from young leaves using a TaKaRa MiniBEST Plant RNA Extraction kit (Takara, Dalian, China), and cDNA was synthesized using PrimeScript™ RT reagent Kit with gDNA Eraser (Takara, Dalian, China).

Evolutionary analysis of the predicted PdPapERF109 protein

To fully understand the evolutionary relationships of the PdPapERF109 protein, 16 gene sequences that encode similar ERF proteins were obtained from the NCBI GenBank database (https://www.ncbi.nlm.nih.gov/) (Stoesser et al. 2014). Using MEGA 5.1 software (Tamura et al. 2011), a neighbor joining (NJ) phylogenetic tree was constructed and the confidence of the branches was estimated using 1,000 iterations of bootstrap resampling and the Poisson model. In addition, to further verify the evolutionary relationships between the ERF proteins, we constructed a second phylogenetic tree using the maximum likelihood (ML) method.

Differential expression of *PdPapERF109* gene

To clarify the role of *PdpapERF109* gene in the process responds to pathogen infection, 6-month-old wild Pdpap were treated with *F. oxysporum* at different stages, and the treatment times were at the beginning, then at 6, 12, 24, and 48 h, respectively. The RNA from each culture was subjected to reverse transcription to obtain first-strand cDNAs. The expression of *PdPapERF109* was analyzed by reverse transcription quantitative real-time PCR (qRT-PCR) performed on a Stratagene Mx3000P real-time PCR system (Agilent Technologies, Santa Clara, USA) using the 2×SYBR Green qPCR Master Mix kit (Bimake, Shanghai, China). The amplification curve was generated after analyzing the raw data. Cycle threshold (Ct) value 0.01 was calculated based on the fluorescence threshold. *Pdpapactin* and *PdpapEF1-α* were used as reference genes to normalize the gene expression (Guo et al. 2021a). The primer sequences for amplifying the reference genes and *PdPapERF109* are in Supplementary Table S2, and the components of the qRT-PCR assays are in Supplementary Table S3. The qRT-PCR amplification conditions were: an initial denaturation of 94 °C for 30 s followed by 44 cycles of 94 °C for 12 s, 58 °C for 30 s, and 72 °C for 45 s, and 79 °C for 1 s. The reaction specificity was determined by performing a melting-curve analysis from 55 ℃ to 99 ℃, with fluorescence readings taken every

0.5 °C for 1 s. The $2^{-\Delta\Delta Ct}$ method (Livak and Schmittgen 2001) was used to calculate the relative expression levels of the target genes, defined as:

$$\Delta\Delta C_t = \left(C_{t-target} - C_{t-control}\right)_2 - \left(C_{t-target} - C_{t-control}\right)_1 \quad (1)$$

where "$C_{t\text{-}control}$" represents the average C_t value of reference genes, "1" represents the untreated group, and "2" represents the treated group. Three biological replicates were performed for each assay.

To determine the spatial expression profiles of the *PdPapERF109* gene, six tissue types were sampled: roots, whole stems, leaves, and the base, middle, and top sections of the stem (~5 cm in length). RNA was extracted from these tissues from 6-month-old wild seedlings. The RNA from each tissue was subjected to reverse transcription to obtain first-strand cDNAs. The expression pattern of *PdpapERF109* gene was analyzed according to the qRT-PCR method described above.

Similarly, the same method was used to analyze the expression level of *PdPapERF109* in transformants. After 2 months, the *PdPapERF109*-overexpressing shoots grown in soil were treated with 20 mL *F. oxysporum* (1×10^5 cfu/mL) by perfusion into the root. The infection time was at 0 h, and 6, 12, 24, and 48 h; each experimental group had three replicates. The transformants were frozen in liquid nitrogen, and total RNA extracted and reverse transcribed to obtain cDNA. The expression level of *PdPapERF109* was determined by qRT-PCR using cDNA as a template from the wild material and transformants for the different pathogen infection times. The primer sequences are given in Supplementary Table S2.

Cloning of the *PdPapERF109* gene and vector construction

PCR cloned the *PdPapERF109* gene using primer sequences (Supplementary Table S4). The components of the PCR amplifications are shown in Supplementary Table S5. The amplification program for PCR was: 94 °C for 3 min followed by 30 cycles of 94 °C for 30 s, 58 °C for 30 s, and 72 °C for 1.5 min, followed by a final extension step of 72 °C for 20 min.

The DNA fragment and the pBI121 overexpression vector were digested with the restriction endonucleases *Xba* I and *Xma* I, and the *PdPapERF109* gene was inserted into pBI121 under control of the cauliflower mosaic virus (CaMV) 35S promoter. The pBI121-*PdPapERF109* recombinant vector was transferred into *Agrobacterium tumefaciens* GV3101 by heat shock transformation (Holsters et al. 1978), and then *Agrobacterium*-mediated transformation was used to introduce the recombinant vector into the Pdpap genome (Guo et al. 2018).

Generating recognized transformant Pdpap plants

Acceptable transformant Pdpap lines were obtained by the leaf disc method (Julia et al. 2017). After cutting the young leaves from 2-month-old Pdpap plants, discs ~ 1 cm diameter were co-cultured with the *Agrobacterium* strain harboring the pBI121-*PdPapERF109* recombinant vector and transferred onto MS differentiation medium containing 50 mg/L kanamycin and 200 mg/L cephalosporin for shoot regeneration. The kanamycin-resistant shoots were rooted on 0.5 × MS medium containing 50 mg/L kanamycin for root regeneration. After selection by kanamycin, acceptable transformants were used for subsequent analysis.

Molecular detection of acceptable transformant Pdpap plants

A DNA extraction kit (Tiangen, Beijing) was used to extract genomic DNA from the acceptable *PdPapERF109*-overexpressing transformed Pdpap plants. PCR detection was performed on DNA extracted from the plants. The pBI121-*PdPapERF109* plasmid as the positive control, wild Pdpap and water as the negative controls. For molecular detection of recombinant vectors, primer pairs pBI121-F were used in the pBI121 vector/*PdPapERF109*-R in the gene sequence, and *PdPapERF109*-F in the gene sequence/pBI121-R in the vector. The PCR primer sequences are given in Supplementary Table S4.

Growth and physiological index measurements

To test resistance to *F. oxysporum* under natural conditions, the wild-type and overexpressing transformant OE4 and OE5 lines were inoculated with *F. oxysporum* and grown in the artificial chamber for 10 days, after which the growth of the plants was assessed. The experiment had three biological replicates. During the experiment, water was added every 3 days to keep the soil moist to avoid the influence of drought.

The survival rates of wild and transformants inoculated with *F. oxysporum* at zero, 5, 10, 15, and 20 days were counted according to Sun et al. (2018). Disease levels were classified according to the following criteria: 0 (no symptoms), 1 (1–25% wilted leaves), 2 (26–50% wilted leaves), 3 (51–75% wilted leaves), and 4 (76–100% wilted leaves) (Xu et al. 2014). The experiment had ten samples. Refer to the following equation (Sun et al. 2018) for calculation:

$$\begin{aligned}\text{Survival Rate} = 1 - 100\% \times [\text{sum (number of plants} \times \text{disease level)}] \\ /[(\text{total number of plants}) \\ \times (\text{maximal disease level})]\end{aligned} \quad (2)$$

The 2-month-old wild material and *PdPapERF109*-overexpressing transformant Pdpap plantlets in the same

growth state were inoculated with *F. oxysporum* and sampled at zero, 5, 10, 15, and 20 days as described above. The value of pathogen inoculation of the wild Pdpap plants at day zero was set to 1. The growth status of each infected plantlet was observed, and fresh weight and root lengths measured. The experiment had three replicates.

The 2-month-old *PdPapERF109*-overexpressing transformants and wild Pdpap plants at similar growth stages were inoculated with *F. oxysporum* and sampled at 0 h, and at 6, 12, 24, 48 h, and 96 h. The inoculated plants were frozen in liquid nitrogen immediately after sampling. Using the methods of Cheng et al. (2020), the samples were used to determine various physiological indicators, including peroxidase (POD) activity, catalase (CAT) activity (Góth 1991), H_2O_2 content, malondialdehyde (MDA) content, and the percentage of electrolyte leakage (Nguyen et al. 2016). The experiment had three replicates.

Antioxidant capability test

Nitroblue tetrazolium chloride (NBT) can detect superoxide activity in plant tissues (Kumar et al. 2013). In order to assess the damage to the leaves by ROS due to *F. oxysporum* infection, the third to sixth leaves of seedlings were sampled 3 days after infection and immediately stained with NBT (Zhou et al. 2020). Dark blue staining indicates that the cells were more damaged by ROS, which means that the antioxidant capacity of the cells was relatively lower.

Statistical analysis

The data were analysed with the Statistical Software Package for Social Science (SPSS) version 17.0. Using the Student's *t*-test to compare the data, $P<0.05$ was considered significantly different. Significant differences ($P<0.05$) are indicated by different lowercase letters.

Results

Phylogenetic analysis

An 809 bp cDNA fragment of the *PdPapERF109* gene was cloned from RNA extracted from wild seedlings. ERF protein sequences like *PdPapERF109* were downloaded and compared. A NJ phylogenetic tree was constructed to show the evolutionary relationships among the sequences. Bootstrap resampling tested the statistical support of the branches. The NJ analysis is shown in Fig. 1A. To test the reliability of the NJ model in detail, the JTT + G + F model was used to build a ML phylogenetic tree using the same data (Fig. 1B). A comparison of the two phylogenetic trees showed that the two models had good consistency, and that *PdPapERF109* shared 100% identify with *ERF109* from *P. trichocarpa* (XM_006384349.2). The PdPapERF109 shared high sequence homology with similar proteins from other species, such as *P. trichocarpa* (100%, LOC18097788, XM_006384349.2), *Lactuca sativa* L. (92.2%, LOC111890860, XM_023886942.1), *Raphanus sativus* L. (91.5%, LOC108816386, XM_018588961.1), *Dendrobium catenatum* Lind. (91.1%, LOC110108677, XM_020839427.2), *Pistacia vera* L. (90.4%,

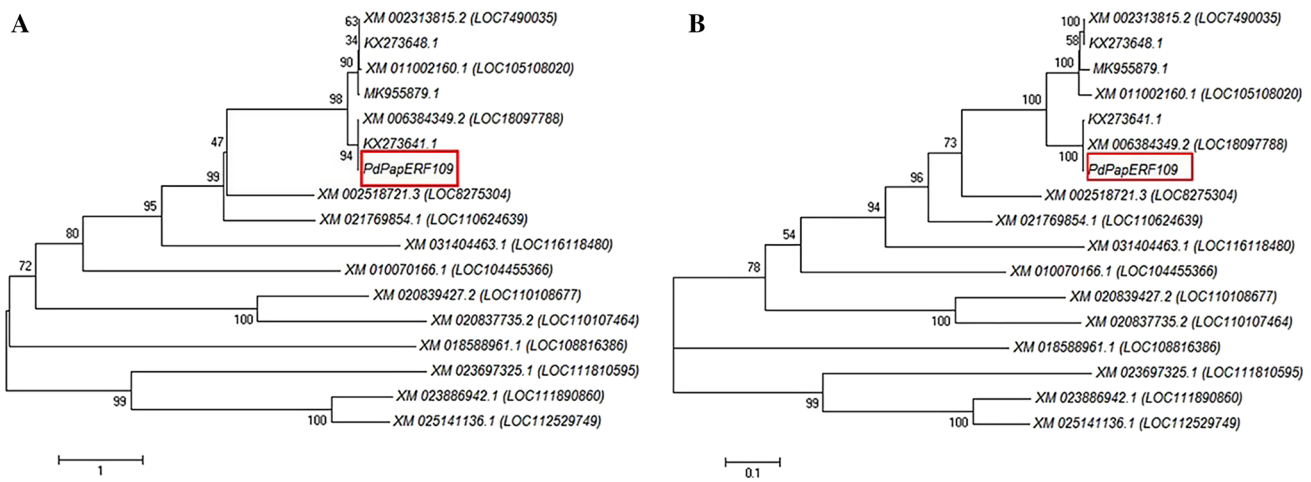

Fig. 1 Dendrogram of *PdPapERF109* and high homology proteins from other species. **A** NJ-phylogenetic tree; **B** ML-phylogenetic tree. Dendrogram was constructed by MEGA5 with neighbor method and Poisson model. *PdPapERF109* was marked with red frame. It showed similar evolutionary relationship under two algorithms

LOC116118480, XM_031404463.1), *Cynara cardunculus* var. *Scolymus* (90.2%, LOC112529749, XM_025141136.1), *Cucurbita pepo* subsp. *Pepo* (86.7%, LOC111810595, XM_023697325.1), *Populus alba* var. *pyramidalis* (85.8%, MK955879.1), *Populus euphratica* (84.8%, LOC105108020, XM_011002160.1), *Ricinus communis* L. (80.3%, LOC8275304, XM_002518721.3), *Manihot esculenta* Crantz (76.3%, LOC110624639, XM_021769854.1) and *Eucalyptus grandis* Hill (76.2%, LOC104455366, XM_010070166.1).

Analysis of differential expression of the *PdPapERF109* gene

After Pdpap seedlings were infected by *F. oxysporum*, the expression of the *PdPapERF109* gene was significantly induced (Fig. 2A). With an extension of infection time, the expression level continued to increase and reached the highest at 48 h after infection.

To determine the spatial expression profiles of the *PdPapERF109* gene, qRT-PCR was used to analyze the expression in different tissues. From the results of this analysis, the expression level is lowest in the leaves and highest in the stems (Fig. 2B). Expression was also compared in different parts of the same tissue, and was lowest in the top part of the stem and highest in the bottom (Fig. 2C).

Molecular detection in putative transformants overexpressing PdPapERF109

After the *PdPapERF109* overexpression vector was transformed into wild Pdpap, five putative transformant lines were obtained. DNA was extracted from leaves of the WT and the five putative transformant Pdpap plants, and PCR was performed using primer pairs pBI121-F/*PdPapERF109*-R and *PdPapERF109*-F/pBI121-R. After PCR amplification, each line gave DNA fragments amplified by both pairs of primers (Fig. 3A). Bands in lanes 1-1 to 5-2 are the same size as bands in lanes "+1" and "+2". A single amplified fragment was detected in each lane, while there were no amplified bands in lanes "− −1", "− −2" and "w−1", "w−2". The gel electrophoresis results show that the size of the amplified target bands from the five putative transformant lines are as expected. The recombinant plasmid (positive control) showed that the gene can be amplified only in the transformants, but not in the wild material, indicating that the pBI121-*PdPapERF109* vector successfully transformed Pdpap, and the five putative transformants contained the *PdPapERF109* gene under the expression of the constitutive CaMV 35S promoter.

Expression analysis of *PdPapERF109* in transformants

As shown in Fig. 4, after inoculation with *F. oxysporum*, wild Pdpap seedlings had wilted and died, but plants of the *PdPapERF109*-overexpression transformants (OE4 and OE5) grew well. There was a slight water loss in leaf blades and petioles of the transformants. The results show that overexpression of the *PdPapERF109* gene in Pdpap plants results in a strong resistance against *F. oxysporum* infection compared to wild plants.

The survival rate showed that, after different infections, the transformants (OE4, OE5) were greater than that of the wild material (Fig. 5A). The fresh weights and root lengths of wild and transformants inoculated at zero (initial step), and at 5, 10, 15, and 20 days were determined, and the values at zero

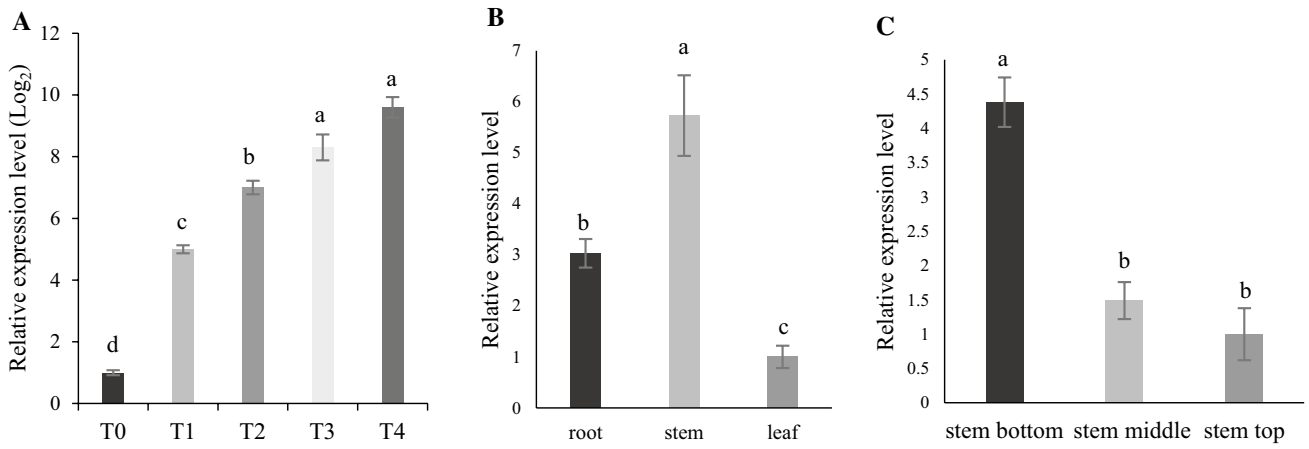

Fig. 2 **A** Analysis of expression patterns of *PapapERF109* gene under different stages of *F. oxysporum* infection; **B** tissue differential expression of *PdPapERF109* in different tissues of Pdpap; **C** tissue differential expression of *PdPapERF109* in different parts of the same tissue. T0–T4: Infection times were 0, 6, 12, 24 and 48 h. Significant differences ($P < 0.05$) are indicated by lowercase letters. Error bars represented standard deviation of three independent replicates

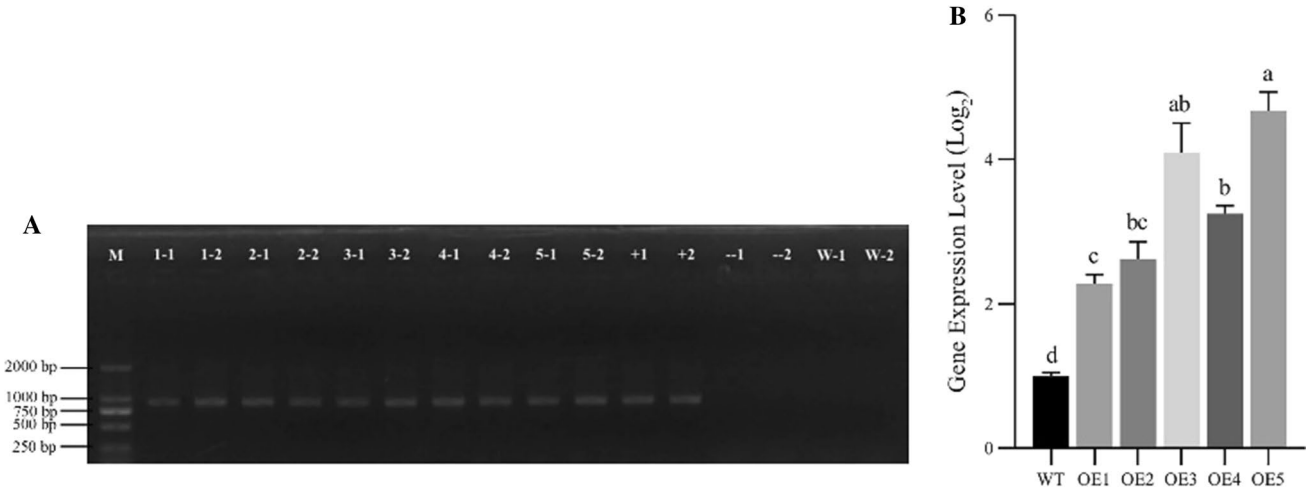

Fig. 3 **A** Molecular detection in overexpressing putative transformant Pdpap of *PdPapERF109*. M: DL 2000 Marker; 1–5: Five overexpressing putative transformant lines were used as amplification templates; +: Positive control using PBI121-*PdPapERF109* plasmid as template; −: Negative control with water as template; W: Negative control with wild-type Pdpap as template; −1: PCR detection of putative transformant lines using PBI121-F and *PdPapERF109*-R as primers; −2: PCR detection of putative transformant lines with *PdPapERF109*-F and PBI121-R as primers. B: Expression level analysis of *PdPapERF109* in transformants. WT: Wild-type Pdpap. OE1–OE5: Transformant lines. Error bars represented standard deviation of three independent replicates. Significant differences ($P<0.05$) were indicated by different lowercase letters

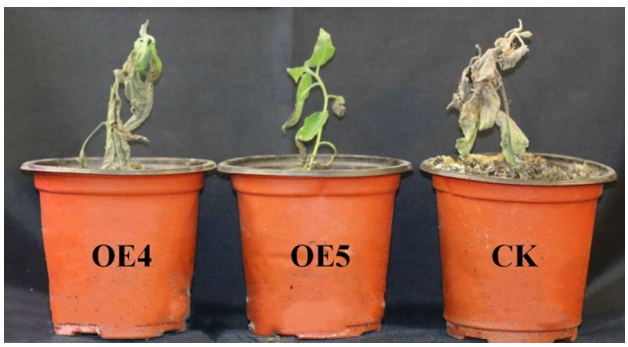

Fig. 4 The growth status of wild Pdpap and overexpressing transformants OE4 and OE5 lines infected by *F. oxysporum* and grown for 10 days. CK: Wild Pdpap, OE4, OE5: Transformant lines

were set to 1. The fresh weights and root lengths are shown in Fig. 5B and C, respectively, and values of the two transformants were consistent with the wild Pdpap plants at D0. In contrast, after *F. oxysporum* infection, the transformants were superior to the wild plants under the same conditions, indicating that they grow better after infection. These results show that ectopic expression of *PdPapERF109* can enhance resistance to *F. oxysporum* during early growth stages in Pdpap plants.

Physiological analysis of transformants infected with *F. oxysporum*

The results of H_2O_2 contents are shown in Fig. 6A. Under normal conditions, the levels in the wild plants were 1.0 ± 0.0 times more than the transformants (OE4, OE5). In plants infected with *F. oxysporum*, the relative differences were 1.3 ± 0.1, 1.3 ± 0.0, 1.3 ± 0.1, 1.2 ± 0.1, and 1.3 ± 0.0 times than those of the transformants after 6, 12, 24, 48, and 96 h. At T0, the H_2O_2 content of the two transformants was basically the same as in the wild Pdpap. However, after *F. oxysporum* infection, H_2O_2 levels in the *PdPapERF109*-overexpressing lines were lower than in the wild plants under the same treatments.

The results of POD activity measurements are shown in Fig. 6B. The experiment had three biological replicates. Under normal conditions, POD activity in the transformants was 1.0 ± 0.0 times greater than in the wild materials. The relative differences in transformants were 1.2 ± 0.0, 1.3 ± 0.0, 1.3 ± 0.1, 1.2 ± 0.1, and 1.5 ± 0.0 times that of the wild Pdpap at 6, 12, 24, 48, and 96 h after infection. From these results, it is shown that at T0, POD activity of the two transformants is basically the same as in the wild plants. After infection, POD activity in the overexpression lines was higher than in wild plants at the same infection times.

Catalase activity is shown in Fig. 6C. Under normal conditions, CAT activity in the OE4 and OE5 transformants was 1.0 ± 0.0 times that of the wild material. After infection by *F. oxysporum*, the relative differences in transformants were 1.1 ± 0.0, 1.1 ± 0.0, 1.2 ± 0.0, 1.1 ± 0.0, and 1.2 ± 0.0

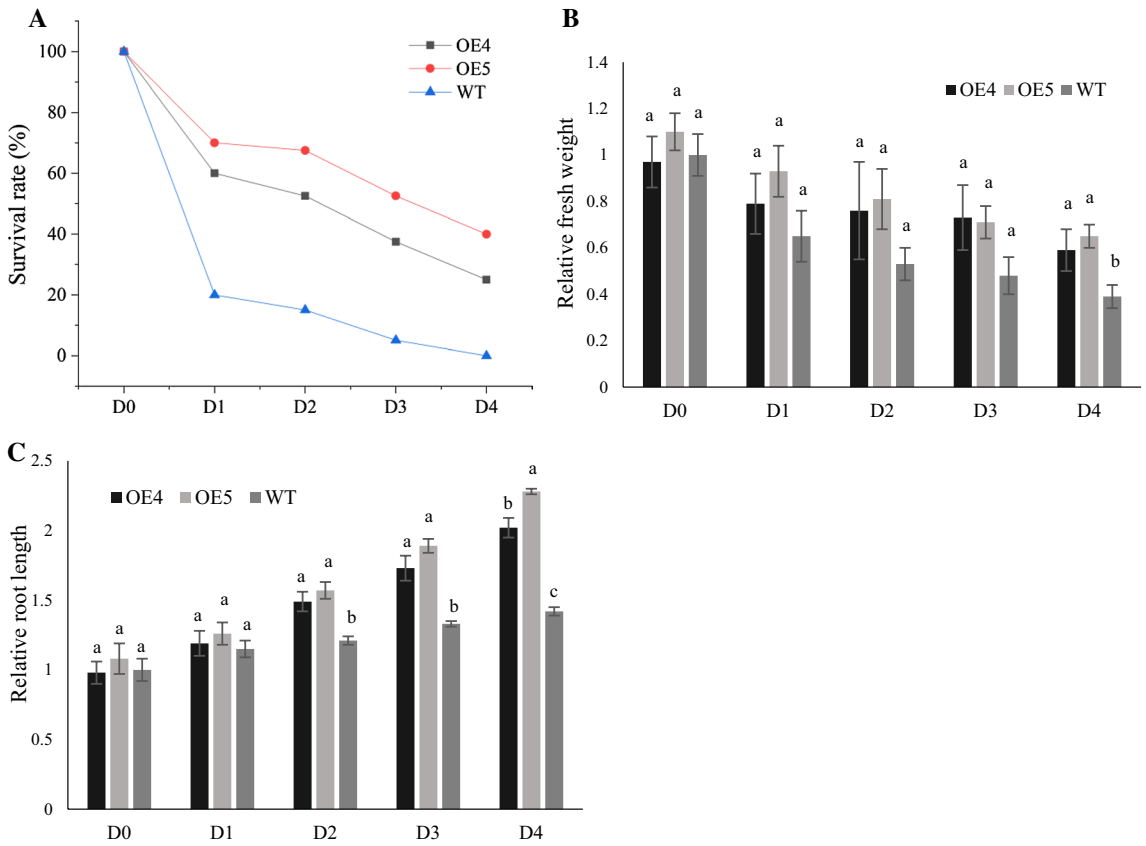

Fig. 5 Morphological characteristics of *PdPapERF109* overexpression transformants. **A**: Survival rate of transformants (OE4 and OE5) and wild Pdpap infected with *F. oxysporum*. **B**: Relative fresh weight of wild Pdpap and transformants treated with *F. oxysporum*; **C**: Root lengths of wild Pdpap and transformants treated with *F. oxysporum*. D0–D4: Infection times were 0, 5, 10, 15 and 20 days. The error bars represent standard deviation of three independent replicates. Significant differences ($P < 0.05$) are indicated by different lowercase letters

times that in wild Pdpap plants at 6, 12, 24, 48, and 96 h. At T0, CAT activity of the two transformants is similar to that of wild plants. However, after *F. oxysporum* infection, CAT activity in the two overexpression lines was higher than in wild Pdpap at the same infection times.

Malondialdehyde (MDA) contents of leaves from wild and transformants were measured (Fig. 6D). Under normal conditions, MDA levels of the transformants were 1.0 ± 0.0 times that of the wild plants. Conversely, the wild plants were 1.2 ± 0.0, 1.3 ± 0.1, 1.3 ± 0.0, 1.4 ± 0.1, and 1.3 ± 0.0 times higher than those of the transformants at 6, 12, 24, 48, and 96 h after infection. At T0, MDA contents of the transformants were essentially the same as that of the wild plants. Following infection, the overexpressing lines had lower malondialdehyde levels than the wild Pdpap plants at the same infection times.

The percentage of electrolyte leakage is shown in Fig. 6E. Under normal conditions, electrolyte leakage in wild plants was 1.1 ± 0.0 times that of the transformants. After infection, the wild plants were 1.4 ± 0.1, 1.4 ± 0.0, 1.4 ± 0.1, 1.4 ± 0.0, and 1.2 ± 0.0 times higher than that of overexpressing lines at 6, 12, 24, 48, and 96 h. At T0, the percentage of electrolyte leakage in the two transformants was basically the same as in wild plants. After infection, the percentage of leakage in the *PdPapERF109*-overexpressing lines was lower than in the wild Pdpap at the same infection times.

Histochemical staining

Infected leaves were stained with nitroblue tetrazolium (NBT) to assess the antioxidant capacity of the transformants (Fig. 7). The staining of the leaves from *PdPapERF109*-overexpressing transformants after infection (Fig. 7C) is slightly darker than in the uninfected wild controls (Fig. 7A), but the overall appearance is similar. In addition, the differences in color compared with leaves of infected wild plants (Fig. 7B) are obvious. These results indicate that in plants infected with *F. oxysporum*, the cells in the transformants show less damage, indicating that they have a greater ability to remove reactive oxygen species (ROS), including O^{2-} and H_2O_2, thereby reducing cell damage and enhancing plant tolerance. This is consistent with POD and CAT activity measurements, and further shows that the

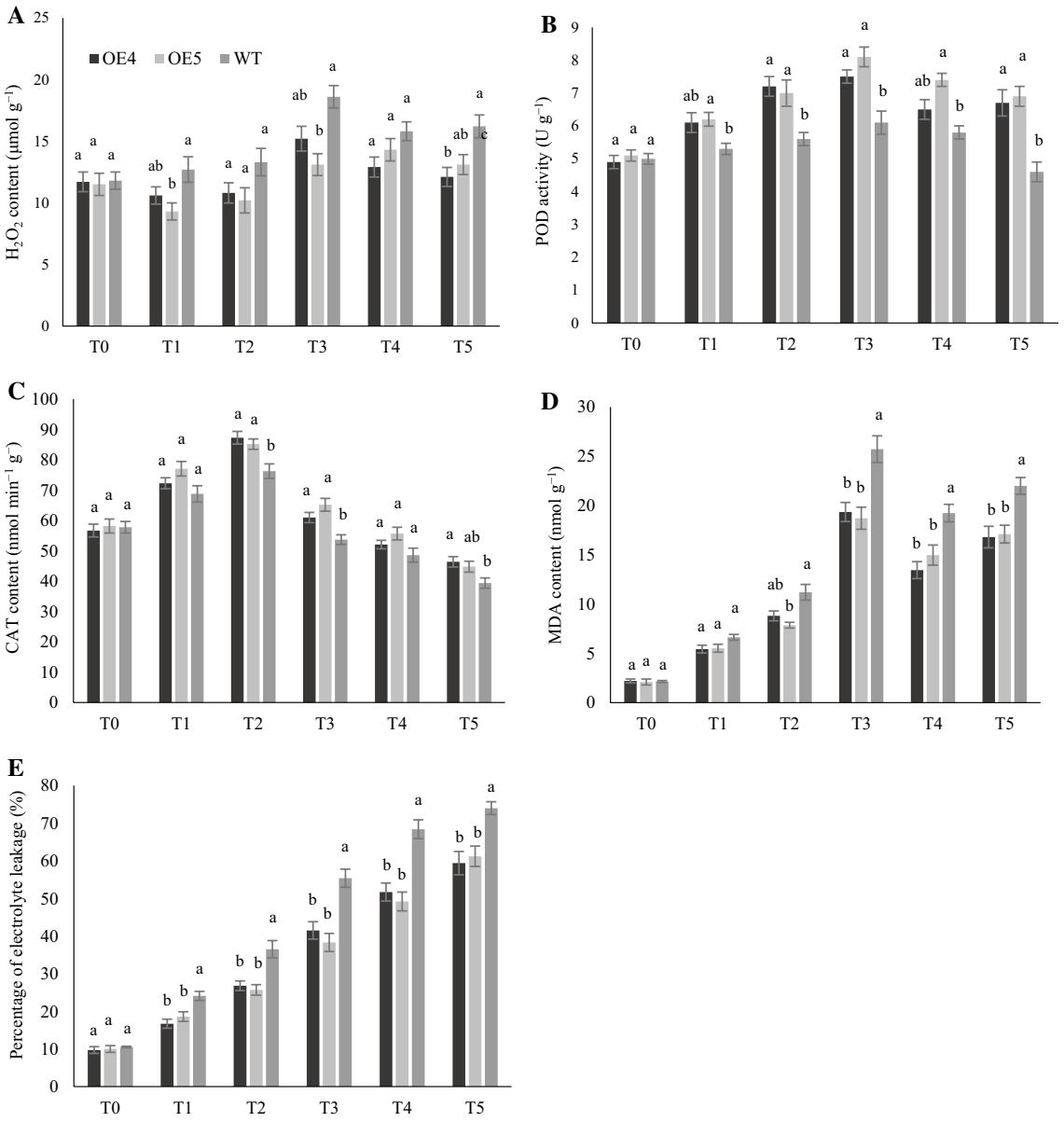

Fig. 6 Physiological characteristic analysis of wild Pdpap and *PdPapERF109* overexpression transformants infected with *F. oxysporum*. Two transformants and WT were used as biological replicates for physiological analysis. **A** Result of H_2O_2 content measurement; **B** Result of POD activity measurement; **C** result of catalase activity; **D** Result of malondialdehyde content; **E** Percentage of electrolyte leakage. T0−T5: Infection times were 0, 6, 12, 24, 48, and 96 h. Error bars represent standard deviation of three independent replicates. Significant differences ($P<0.05$) are indicated by different lowercase letters

overexpression of *PdPapERF109* in Pdpap plants reduces the accumulation of intracellular ROS. Overexpression effectively enhances the antioxidant capacity of the plants, thus improving the resistance of Pdpap to *F. oxysporum* infection.

Discussion

Transcription factors play an important role in abiotic and biological stress responses (Akhtar et al. 2012). TF families such as WRKY, AP2/ERF, NAC, bZIP, and MYB (Pu et al. 2019) affect stress tolerance by regulating downstream response genes (Joshi et al. 2016). Members of the ERF family play a critical role in the responses to stresses, including pathogenic microorganism infection (Guo et al. 2016), ion concentration damage (Yang et al. 2018), excess water or drought (Labbo et al. 2018), and temperature stress (Licausi et al. 2013). At the same time, in the process of defending against stress, the regulation of jasmonic acid, abscisic acid, and ethylene pathways will be integrated (Müller and Bosch

Fig. 7 Results of superoxide staining by NBT. **A** Leaves of wild PdPap without treatment; **B** Leaves of wild PdPap with *F. oxysporum*; **C** Leaves of overexpressing transformants with *F. oxysporum*. Staining intensities of WT without treatment and transformants infected by *F. oxysporum* are similar, but greatly increased in WT treated by *F. oxysporum*

2015). The results of Yi et al. (2004) showed that ERF family genes produce resistance responses to various pathogens during heterologous expression of plants, which can promote the activation of related resistance pathways, thereby effectively reducing the damage to plants exposed to stress.

Previous studies have shown that the *PdPapERF109* gene plays a positive role in various biological and abiotic stresses. There are several reports on the resistance functions of the *PdPapERF109* gene in salt stress (Bahieldin et al. 2018), low temperature stress (Wang et al. 2019) and drought resistance (Shi et al. 2015), and these studies have established a foundation for our early prediction and subsequent verification experiments. Research has shown that the JA-responsive ethylene response factor 109 (*ERF109*) mediates crosstalk between JA signaling and auxin biosynthesis to regulate lateral root formation in *Arabidopsis* (Cai et al. 2014). This indicates that the *PdPapERF109* gene may regulate the formation of lateral roots in Pdpap to achieve an effective response after infection by *F. oxysporum*.

In this study, differential expression levels for *PdPpapERF109* in recognized transformants may be due to different copy numbers and sites of insertion. The overexpression of the gene plays a significant role in the growth and physiological state of plants after pathogen infection. The results indicate that the *PdPapERF109* gene plays a role in signaling pathways under stress conditions.

One of the important mechanisms of plant disease resistance is the change and increase in the activities of defense-related enzymes (Gong et al. 2010). By measuring the malondialdehyde content and the percentage of electrolyte leakage, the relative degree of damage to the plant cell membranes can be quantified. The determination of physiological indexes such as H_2O_2 contents, CAT levels, and POD activity can provide a detailed understanding of the ability of the *PdPapERF109*-overexpressing transformants to remove ROS from the cells and their antioxidant capacity. Studies have shown that different rapeseed varieties express different degrees of resistance to black shank disease, and these resistance capabilities are reflected in a significant increase in the level of POD activity (Peng et al. 2015). *Trichoderma aculeatus* resists tomato wilt caused by *F. oxysporum* by increasing the activity of different defense enzymes, thereby improving the disease resistance of tomatoes (Patel and Saraf 2017). In this study, we measured the physiological indicators of the *PdPapERF109*-overexpressing transformants, including H_2O_2, POD, CAT, MDA, and the percentage of electrolyte leakage. The purpose of these experiments was to evaluate the resistance of Pdpap plants through the changes in the activities of defense-related enzymes.

NBT staining showed that the overexpression of *PdPapERF109* effectively reduced the accumulation of ROS in plants infected with *F. oxysporum*.

According to previous research, key transcription factors can positively regulate the expression levels of SOD and POD genes, thereby enhancing their activity for removing ROS (Zhao et al. 2019; Guo et al. 2021b). It is also believed that under stress conditions, key transcription factors promote the production of POD and SOD through physiological or biochemical reactions, thereby promoting the removal of ROS (Cheng et al. 2020). Based on the previous reports, it is speculated that under normal conditions, the *PdPapERF109* gene will not directly increase POD and CAT contents in the overexpressing transformants. Similarly, the content of ROS did not change significantly in Pdpap. However, in response to *F. oxysporum* infection, expression of the *PdPapERF109* gene can promote the production of POD and CAT through the action of the PdpapERF109 transcription factor on gene expression, thereby promoting the removal of ROS. Therefore, under normal conditions, there is no significant differences in physiological changes between wild plants and transformants. Our data indicates that the *PdPapERF109* gene may play an important role in ROS clearance to protect the plant from external stresses. In addition, the molecular mechanism of gene regulation and the gene network related to *PdPapERF109* expression in response to *F. oxysporum* infection requires further study.

Conclusion

In this study, we cloned a transcription factor gene, *PdpapERF109*, from Pdpap. Subsequently, overexpressing transgenic lines were obtained in Pdpap. The results of morphological and physiological analyses showed that overexpressing transgenic lines were significantly resistant to *F. oxysporum* compared with WT. Further studies showed that *PdpapERF109* could enhance the ROS scavenging ability of Pdpap under stress. Therefore, we concluded that *PdpapERF109* has an important regulatory role during the stress response to *F. oxysporum*.

References

Akhtar M, Jaiswal A, Taj G, Jaiswal JP, Qureshi MI, Singh NK (2012) DREB1/CBF transcription factors: their structure, function and role in abiotic stress tolerance in plants. J Genet 91:385–395

Ali MA, Abbas A, Kreil DP, Bohlmann H (2013) Overexpression of the transcription factor RAP2.6 leads to enhanced callose deposition in syncytia and enhanced resistance against the beet cyst nematode *Heterodera schachtii* in Arabidopsis roots. BMC Plant Biol 13:47–64

Bahieldin A, Atef A, Edris S, Gadalla NO, Ramadan AM, Hassan SM, Al-Attas SG, Al-Kordy MA, Al-Hajar ASM, Sabir JSM, Nasr ME, Osman GH, El-Domyati FM (2018) Multifunctional activities of *ERF109* as affected by salt stress in *Arabidopsis*. Sci Rep 8:6403–6413

Bootsma HJ, Heide HGJ, Pas S, Schouls LM, Mooi FR (2000) Analysis of *Moraxella catarrhalis* by DNA typing: evidence for a distinct subpopulation associated with virulence traits. J Infect Dis 181:1376–1387

Cai XT, Xu P, Zhao PX, Liu R, Yu LH, Xiang CB (2014) Arabidopsis *ERF109* mediates cross-talk between jasmonic acid and auxin biosynthesis during lateral root formation. Nat Commun 5:5833–5846

Chen NN, Tong SF, Tang H, Zhang ZY, Liu B, Lou SL, Liu JQ, Liu HH, Ma T, Jiang YZ (2020) The PalERF109 transcription factor positively regulates salt tolerance via *PalHKT1;2* in *Populus alba* var. *pyramidalis*. Tree Physiol 40:6–24

Cheng ZH, Zhang XM, Zhao K, Zhou BR, Jiang TB (2020) Ectopic expression of a poplar gene *NAC13* confers enhanced tolerance to salinity stress in transgenic *Nicotiana tabacum*. J Plant Res 133:727–737

Cossu RM, Buti M, Giordani T, Natali L, Cavallini A (2012) A computational study of the dynamics of LTR retrotransposons in the *Populus trichocarpa* genome. Tree Genet Genomes 8:61–75

Diao J, Wang JQ, Zhang P, Hao X, Wang Y, Liang LW, Zhang Y, Ma W, Ma L (2021) Transcriptome analysis reveals the important role of *WRKY28* in *Fusarium oxysporum* resistance. Front Plant Sci 12:720679

Dossa K, Wei X, Li DH, Fonceka D, Zhang YX, Wang LH, Yu JY, Liao BS, Diouf D, Cissé N, Zhang XR (2016) Insight into the AP2/ERF transcription factor superfamily in sesame and expression profiling of DREB subfamily under drought stress. BMC Plant Biol 16:171–187

Florendo PDC, Roxas DB, Robles AY, Aquino DL, Abella MP (2003) Influence of plant cell wall composition and degradation on the feed intake, nutrient digestibility, and milk production of buffaloes at mid-lactation. PCARRD Highlights 24:1873–1878

Fujimoto SY, Ohta M, Usui A, Shinshi H, Takagi MO (2000) *Arabidopsis* ethylene-responsive element binding factors act as transcriptional activators or repressors of GCC box-mediated gene expression. Plant Cell 12:393–404

Gong DQ, Gu H, Zhang LB, Wang SB, Zhan RL, Zhu SJ (2010) Effects of benzothiadiazole on disease resistance and related defense enzyme activity of harvested mango fruits. Int J Fruit Sci 27:585–590 (**in Chinese**)

Góth L (1991) A simple method for determination of serum catalase activity and revision of reference range. Clin Chim Acta 196:143–151

Guo WF, Jin L, Miao YH, He X, Hu Q, Guo K, Zhu LF, Zhang XL (2016) An ethylene response-related factor, *GbERF1-like*, from *Gossypium barbadense* improves resistance to *Verticillium dahliae* via activating lignin synthesis. Plant Mol Biol 91:305–318

Guo RT, Wang ZY, Huang Y, Fan HJ, Liu ZH (2018) Biocontrol potential of saline- or alkaline-tolerant *Trichoderma asperellum* mutants against three pathogenic fungi under saline or alkaline stress conditions. Braz J Microbiol 49:236–245

Guo RT, Wang ZY, Zhou C, Huang Y, Fan HJ, Wang YC, Liu ZH (2020) Biocontrol potential of *Trichoderma asperellum* mutants T39 and T45 and their growth promotion of poplar seedlings. J for Res 31(3):1035–1043

Guo Q, Jiang JH, Yao WJ, Li L, Zhao K, Cheng ZH, Han LB, Wei R, Zhou BR, Jiang TB (2021a) Genome-wide analysis of poplar HD-Zip family and over-expression of PsnHDZ63 confers salt tolerance in transgenic *Populus simonii* × *P. nigra*. Plant Sci 311:111021

Guo RT, Ji SD, Wang ZY, Zhang HF, Wang YC, Liu ZH (2021b) *Trichoderma asperellum* xylanases promote growth and induce resistance in poplar. Microbiol Res 248:126767

Holsters M, Waele D, Depicker A, Messens E, Montagu M, Schell J (1978) Transfection and transformation of *Agrobacterium tumefaciens*. Mol Gen Genet 163:181–187

Hou LH, Cao XQ, Wang C, Lu M (2009) Effect of overexpression of transcription factors on the fermentation properties of *Saccharomyces cerevisiae* industrial strains. Lett Appl Microbiol 49:14–19

Huang JS (2001) Fortification of plant cell walls as a resistance mechanism. Plant Pathog Resist 8:485–524

Ikeda K, Sakai H, Urushibara T, Shibata S, Shiraishi T, Yanagisawa K, Tsuchiya M (2005) The present state and occurrence cause of root rot disease of black pepper caused by *Fusarium solani* f. sp. piperis in the north of the State of Para in Brazil-(Abstracts of the papers presented at the 2005 annual meeting in Shizuoka, 139). Ann Phytopathol Soc JPN 71:25–44

Jin LG, Li H, Liu JY (2010) Molecular characterization of three novel ethylene responsive 2 element binding factor genes from cotton. J Integr Plant Biol 52:485–495

Joshi R, Wani SH, Singh B, Bohra A, Dar ZA, Lone AA, Pareek A, Pareek SSL (2016) Transcription factors and plant response to drought stress: Current understanding and future directions. Front Plant Sci 7:1029–1039

Julia N, Matthias F, Tobias B, Becker D (2017) Old methods rediscovered: application and improvement of two direct transformation methods to hybrid poplar (*Populus tremula* × *P. alba*). Plant Cell Tissue Org 130:183–196

Kagaya Y, Ohmiya K, Hattori T (1999) RAV1, a novel DNA-binding protein, binds to bipartite recognition sequence through two distinct DNA-binding domains uniquely found in higher plants. Nucleic Acids Res 27:470–478

Köppl C, Carr CE (2003) Computational diversity in the cochlear nucleus angularis of the *Barn Owl*. J Neurophysiol 89:2313–2329

Kumar D, Yusuf MA, Singh P, Sardar M, Sarin NB (2013) Modulation of antioxidant machinery in α-tocopherol-enriched transgenic *Brassica juncea* plants tolerant to abiotic stress conditions. Protoplasma 250:1079–1089

Labbo AM, Mehmood M, Akhtar MN, Khan MJ, Tariq A, Sadiq I (2018) Genome-wide identification of AP2/ERF transcription factors in mungbean (*Vigna radiata*) and expression profiling of the *VrDREB* subfamily under drought stress. Crop Pasture Sci 69:1009–1019

Li MT, Zhang SS (2010) Induction of extracellular cell wall-degrading enzymes from *Fusarium oxysporum f. sp. cubense* and their effect on degradation of banana tissue. Chin Agric Sci Bull 5:228–231

Licausi F, Takagi MO, Perata P (2013) APETALA2/Ethylene Responsive Factor (AP2/ERF) transcription factors: mediators of stress responses and developmental programs. New Phytol 199:639–649

Livak KJ, Schmittgen TD (2001) Analysis of relative gene expression data using real-time quantitative PCR and the $2^{-\Delta\Delta CT}$ method. Methods 25:402–408

Lu JH, Liu J, Yan L (2004) The study on soluble salt ions content in different parts of *Populus alba* L. var. *pyramidalis*. J Inner Mongolia Inst Agric Animal Husb 1:25–30 (**in Chinese**)

Lu YW, Wang GQ, Meng QJ, Zhang WH (2011) Effects of enhanced temperature on chlorophyll content and chlorophyll fluorescence parameters in *Populus tomentosa Carr*. J Henan Agr Sci 10:115–119 (**in Chinese**)

Ma LJ, Geiser DM, Proctor RH, Rooney AP, Donnell KO, Trail F, Gardiner DM, Manners JM, Kazan K (2013) *Fusarium* pathogenomics. Annu Rev Microbiol 67:399–416

Mader MM, Cameron DA (2006) Effects of induced systemic hypothyroidism upon the retina: regulation of thyroid hormone receptor alpha and photoreceptor production. Mol vis 12:915–930

Maheshwari P, Kovalchuk I (2016) *Agrobacterium*-mediated stable genetic transformation of *Populus angustifolia* and *Populus balsamifera*. Front Plant Sci 7:296–308

Makkar HPS, Siddhuraju P, Becker K (2007) Plant secondary metabolites. Methods Mol Biol 393:1–122

Miedes E, Suslov D, Vandenbussche F, Kenobi K, Ivakov A, Straeten DVD, Lorences EP, Mellerowicz E, Verbelen JP, Vissenberg K (2013) Xyloglucan endotransglucosylase /hydrolase (XTH) overexpression affects growth and cell wall mechanics in etiolated *Arabidopsis* hypocotyls. J Exp Bot 64:2481–2497

Mizoi J, Shinozaki K, Shinozaki YS (2012) AP2/ERF family transcription factors in plant abiotic stress responses. BBA - Gene Regul Mech 1819:86–96

Moncrief IR (2010) Efforts to characterize the genome organization and gene expression patterns of the cotton root rot fungus, *Phymatotrichopsis Omnivora*. Diss Theses - Gradworks 2:105–128

Müller M, Bosch SM (2015) Ethylene response factors: a key regulatory hub in hormone and stress signaling. Plant Physiol 169:32–41

Nguyen KH, Ha CV, Nishiyama R, Watanabe Y, González MAL, Fujita Y, Tran UT, Li WQ, Tanaka M, Seki M, Schaller GE, Estrella LH, Tran LS (2016) Arabidopsis type B cytokinin response regulators ARR1, ARR10, and ARR12 negatively regulate plant responses to drought. P Natl Acad Sci USA 113:3090–3095

Ning K, Ding CJ, Zhu WX, Zhang WX, Dong YF, Shen YB, Su XH (2018) Comparative metabolomic analysis of the cambium tissue of non-transgenic and multi-gene transgenic Poplar (*Populus* × *euramericana* 'Guariento'). Front Plant Sci 9:1201

Patel S, Saraf M (2017) Biocontrol efficacy of *Trichoderma* asperellum MSST against tomato wilting by *Fusarium oxysporum* f. sp. *lycopersici*. Archiv Fr Pflanzenschutz 50:228–238

Peng SC, Yang P, Zheng L, Cai HB, Guan Y (2015) Resistance Identification of different flue-cured tobacco varieties against black shank. Plant Dis Pests Z1:15–18

Pu YY, Liu LJ, Wu JY, Zhao YH, Bai J, Ma L, Yue JL, Jin JJ, Niu ZX, Fang Y, Sun WC (2019) Transcriptome profile analysis of winter rapeseed (*Brassica napus* L.) in response to freezing stress, reveal potentially connected events to freezing stress. Int J Mol Sci 11:20–24

Puhalla JE (2011) Classification of strains of *Fusarium oxysporum* on the basis of vegetative compatibility. Can J Bot 63:179–183

Qin HX, Jia ZP, Zhang HC, Liu JM, Song YX (2005) Isolation and characterization of a DRE-binding transcription factor from *Yinxin Poplar* (*Populus alba* × *P. alba* var. *pyramidalis*). Chin J Biotechnol 21:906–910 (**in Chinese**)

Qiu WM, Zhu AD, Wang Y, Chai LJ, Ge XX, Deng XX, Guo WW (2012) Comparative transcript profiling of gene expression between seedless *Ponkan mandarin* and its seedy wild type during floral organ development by suppression subtractive hybridization and cDNA microarray. BMC Genom 13:397–414

Qu YP, Kang SZ, Wang SF (2014) Study on water consumption of irrigated *Populus alba* var. *pyramidalis* in Shiyang River Basin. J Chin Inst Water Resour Hydr Res 2:130–137 (**in Chinese**)

Sakuma Y, Liu Q, Dubouzet JG, Abe H, Shinozaki K, Shinozaki KY (2002) DNA-binding specificity of the ERF/AP2 domain of *Arabidopsis* DREBs, transcription factors involved in dehydration- and cold-inducible gene expression. Biochem Bioph Res Commun 290:998–1009

Shi QL, Dong YB, Qiao DH, Wang QL, Ma ZY, Zhang FF, Zhou Q, Xu H, Deng F, Li YL (2015) Isolation and characterization of *ZmERF1* encoding ethylene responsive factor-like protein 1 in popcorn (*Zea mays L.*). Plant Cell Tissue Org 120:747–756

Stangarlin JR, Kuhn OJ, Toledo MV, Portz RL, Schwanestrada KRF, Pascholati SF (2011) The plant defense against pathogens. Sci Ag Paranaensis 6:18–46

Stein U, Jürchott K, Walther W, Bergmann S, Schlag PM, Royer HD (2001) Hyperthermia-induced nuclear translocation of transcription factor YB-1 leads to enhanced expression of multidrug resistance-related ABC transporters. J Biol Chem 276:28562–28569

Stoesser G, Griffith M, Griffith OL (2014) NCBI (National Center for Biotechnology Information). Am Cancer Soc 4:126–136

Sun LF, Xing SC, Zhang J, Yang JF, Wang XZ, Dong YS (2009) Function of the transcription factors in plant domestication and stress resistance. Genom Appl Biol 3:569–577 (**in Chinese**)

Sun LF, Qin J, Rong W, Ni H, Guo HS, Zhang J (2018) Cellophane surface-induced gene, *VdCSIN1*, regulates hyphopodium formation and pathogenesis via cAMP-mediated signalling in *Verticillium dahliae*. Mol Plant Pathol 10:12756

Takagi MO, Suzuki K, Shinshi H (2020) Regulation of ethylene-induced transcription of defense genes. Plant Cell Physiol 41:1187–1192

Tamura K, Peterson D, Peterson N, Stecher G, Nei M, Kumar S (2011) MEGA5: molecular evolutionary genetics analysis using maximum likelihood, evolutionary distance, and maximum parsimony methods. Mol Biol Evol 28:2731–2739

Wang H, Ng TB (1999) Pharmacological activities of fusaric acid (5-butylpicolinic acid). Life Sci 65:849–856 (**in Chinese**)

Wang M, Dai WS, Du J, Ming RH, Dahro B, Liu JH (2019) *ERF109* of trifoliate orange (*Poncirus trifoliata* (L.) Raf.) contributes to cold tolerance by directly regulating expression of *Prx1* involved in antioxidative process. Plant Biotechnol J 17:1316–1332

Wasternack C, Strnad M (2019) Jasmonates are signals in the biosynthesis of secondary metabolites—PATHWAYS, transcription factors and applied aspects—a brief review. New Biotechnol 48:1–11

Wu HS, Wang Y, Zhang CY, Gu M, Liu YX, Chen G, Wang JH, Tang Z, Mao ZS, Shen QR (2009) Physiological and biochemical responses of in vitro *Fusarium oxysporum* f. sp. niveum to benzoic acid. Folia Microbiol 54:115–122

Xie BD, Ma BH, Hu XZ, Li XT (1993) A study on the wilt disease of *Populus* × *euramericana*. J Cent South for Univ 1:25–33 (**in Chinese**)

Xu L, Zhang WW, He X, Liu M, Zhang K, Shaban M, Sun LQ, Zhu JC, Luo YJ, Yuan DJ, Zhang XL, Zhu LF (2014) Functional characterization of cotton genes responsive to *Verticillium dahliae*

through bioinformatics and reverse genetics strategies. J Exp Bot 65:6679–6692

Xue GP, Loveridge CW (2010) HvDRF1 is involved in abscisic acid-mediated gene regulation in barley and produces two forms of AP2 transcriptional activators, interacting preferably with a CT-rich element. Plant J 37:326–339

Yang RC, Liu J, Lin Z, Sun W, Wu ZW, Hu HQ, Zhang YQ (2018) ERF transcription factors involved in salt response in tomato. Plant Growth Regul 84:1–10

Yao ZH, Baloch AM, Liu ZH, Zhai TT, Jiang CY, Liu ZY, Zhang RS (2018) Cloning and characterization of an aux/iaa gene in *Populus davidiana* × *P. Alba* var. *pyramidalis* and the correlation between its time-course expression and the levels of indole-3-acetic in saplings inoculated with *trichoderma*. Pak J Bot 50:169–177

Yi SY, Kim JH, Young YH, Lee S, Kim WT, Yu SH, Choi D (2004) The pepper transcription factor CaPF1 confers pathogen and freezing tolerance in *Arabidopsis*. Plant Physiol 136:2862–2874

Yu WJ, Yang S, Diao GP (2019) Effect of *Trichoderma atroviride* on growth and disease resistance of *Populus davidiana* × *P. alba* var. *pyramidalis*. J Northeast for Univ 1:71–75 (**in Chinese**)

Zadworna AB, Barakat A, Akomy P, Smoliński DJ, Zadworny M (2014) Lignin and lignans in plant defence: Insight from expression profiling of cinnamyl alcohol dehydrogenase genes during development and following fungal infection in *Populus*. Plant Sci 229:111–121

Zeng FK, Mu ZL (2016) Research on field experiment of the *Cantilevered Scaffold* in high-rise building. J Qingdao Agr Univ 4:325–332 (**in Chinese**)

Zhang HM, Xia XL, Yin WL (2009) Tissue culture and rapid propagation of *Populus trichocarpa* Torr. & Gray. Plant Physiol Commun 1:53–54 (**in Chinese**)

Zhao ZM, Chi R, Yang SZ, Wang YJ (2015) Cold resistance of hybrid poplar for *Sect. Populus*. Prot Forest Sci Technol 9:42–43 (**in Chinese**)

Zhao K, Zhang DW, Zhang XM, Cheng ZH, Li RH, Zhou BR, Jiang TB (2019) Functional characterization of poplar *WRKY75* in salt and osmotic tolerance. Plant Sci 289:110259

Zhou C, Guo RT, Ji SD, Fan HJ, Wang JJ, Wang YC, Liu ZH (2020) Isolation of *Trichoderma* from forestry model base and the antifungal properties of isolate TpsT17 toward *Fusarium oxysporum*. Microbiol Res 231:126371

Zorrilla JMF, Vidriero IL, Carrasco JL, Godoy M, Vera P, Solano R (2014) DNA-binding specificities of plant transcription factors and their potential to define target genes. Proc Natl Acad Sci USA 111:2367–2372